Journal of Clinical and Translational Research 2024; 10(3): 212-218

Journal of Clinical and Translational Research

Journal homepage: http://www.jctres.com/en/home

ORIGINAL ARTICLE

Development and validation of an *ex vivo* porcine model of functional tricuspid regurgitation

Hannah Rando*, Rachael Quinn, Emily L. Larson, Zachary Darby, Ifeanyi Chinedozi, Jin Kook Kang, Gyeongtae Moon, James S. Gammie

Johns Hopkins University School of Medicine, Baltimore, Maryland, United States of America

ARTICLE INFO

Article history:
Received: January 28, 2024
Accepted: March 21, 2024
Published Online: June 5, 2024

Keywords:
Ex vivo
Functional tricuspid regurgitation
Porcine
Translational

**Corresponding author:*
Hannah Rando
Johns Hopkins University School of Medicine, Baltimore, Maryland, United States of America.
Email: hrando1@jh.edu

ABSTRACT

Background and Aim: *Ex vivo* models of functional tricuspid regurgitation (FTR) are needed for pre-clinical testing of novel surgical and interventional repair strategies, but current options are costly or have not been formally validated. The objective of this research was to create and validate an *ex vivo* model to test novel repair methods for FTR.

Methods: In explanted porcine hearts, the right atrium was excised to visualize the tricuspid valve. The pulmonary artery and aorta were clamped and cannulated, the coronary arteries ligated, and the right and left ventricles statically pressurized with air to 30 mmHg and 120 mmHg, respectively. FTR was induced by increasing right ventricular pressure to 80 mmHg for 3 h, which resulted in progressive tricuspid annular enlargement, right ventricular dilation, papillary muscle displacement, and central tricuspid malcoaptation. A structured light scanner was used to image the 3D topography of the tricuspid valve in both the native and FTR state, and images were exported into scan-to-computer-aided design software, which allowed for high-resolution 3D computational reconstruction. Relevant geometric measurements were sampled including annular circumference and area, major and minor axis diameter, and tenting height, angle, and area. Geometric measurements from the *ex vivo* model were compared to clinical transthoracic echocardiographic (TTE) measurements using two-sample *t*-tests.

Results: A total of 12 porcine hearts were included in the study. Annular measurements of the native valve were comparable to published TTE data, except for the minor axis diameter, which was shorter in the *ex vivo* model (2.5 vs. 3.1 cm, $P = 0.007$). Induction of FTR in the *ex vivo* model resulted in annular enlargement (FTR vs. native: circumference 13.7 vs.11.8 cm, $P = 0.012$; area 14 vs. 11 cm^2, $P = 0.011$). *Ex vivo* leaflet measurements in both the native and FTR model differed from published TTE data, but demonstrated comparable directional changes between the native and regurgitant states, including increased tenting height, area, and volume.

Conclusion: The *ex vivo* pneumatically-pressurized porcine model closely recapitulates the geometry of both the native and regurgitant tricuspid valve complex in humans and holds promise for testing novel FTR repair strategies.

Relevance for Patients: Currently available interventions for the tricuspid valve have a risk of permanent conduction abnormalities and are insufficient in addressing tricuspid disease for a subset of patients. This *ex vivo* model provides a platform for testing of novel interventions that address the deficiencies of current tricuspid therapies.

1. Introduction

Functional tricuspid regurgitation (FTR) is the most prevalent tricuspid valve abnormality and refers to regurgitation that occurs in the absence of leaflet abnormalities [1]. The most common repair strategy for FTR is tricuspid annuloplasty, but this strategy carries a risk of conduction abnormalities requiring permanent pacemaker implantation and is

DOI: https://doi.org/10.36922/jctr.24.00003

not uniformly effective for patients with massive or torrential FTR and/or those with significant leaflet tethering [2]. For these reasons, a novel surgical or percutaneous repair option that addresses these shortcomings would be of significant value.

To test novel therapies for FTR, an *ex vivo* model of FTR is needed. Unfortunately, the currently available *ex vivo* models of the tricuspid valve are costly, difficult to replicate, or have not been formally validated [3-8]. Our laboratory has previously been successful in developing an *ex vivo* model of secondary mitral regurgitation (SMR) using isolated porcine hearts [9]. Given the comparable tricuspid anatomy between humans and swine [5-8,10] we hypothesized that porcine hearts could similarly be used to develop a static *ex vivo* model of FTR.

2. Materials and Methods

2.1. Ex vivo model setup

Isolated porcine hearts were procured from an abattoir (ATSCO, Inc, Plano, TX, USA), and any remaining pericardium was removed. The coronary arteries were ligated using a 2-0 silk suture, and the aorta and pulmonary artery were cross-clamped. Cannulae were placed into the pulmonary artery and aorta through purse string sutures and were advanced into the right ventricle and left ventricle, respectively. Pressurized air was delivered through the cannulae using a 38-W linear-drive air pump (Thomas, Gardner-Denver Medical, Sheboygan, WI, USA), and ventricular pressure was maintained at 120 mmHg in the left ventricle, and 30 mmHg in the right ventricle. Static pressurization of the left ventricle and right ventricle in such a manner results in the closure of the mitral and tricuspid valves and allows for assessment of valvular geometry (Figure 1). The right atrium was then opened and the atrial tissue was retracted laterally to allow for subsequent imaging and manipulation of the tricuspid valve (Figure 2A).

2.2. Image acquisition

A three-dimensional (3D) structured light scanner (Artec 3D, Luxembourg) was used to capture the shape and texture of the tricuspid valve surface. The scanner generates a 3D model of the tricuspid valve by projecting light onto the valvular surface and recording the pattern of light reflected back to the scanner. The light distortions caused by the surface structures of the tricuspid valve can be analyzed to generate a 3D point cloud. The point cloud is then exported into a 3D scan-to-computer-aided design reverse engineering software (Geomagic, Morrisville, North Carolina, USA), which allows for visualization of the tricuspid valve as a 3D model and enables subsequent analysis of the valvular geometry (Figure 3).

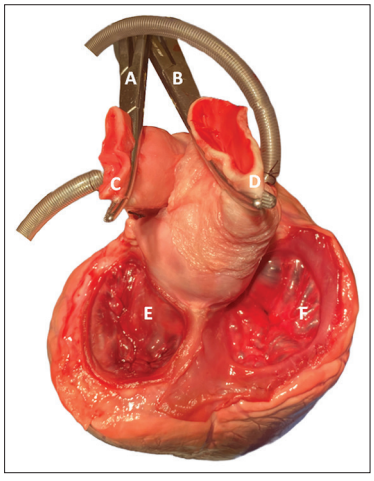

Figure 1. Pneumatic *ex vivo* model of the tricuspid valve with pulmonary artery cross-clamp (A), aortic cross-clamp (B), cannulated pulmonary artery (C), cannulated aorta (D), mitral valve (E), and tricuspid valve (F).

2.3. Induction of FTR

After imaging the tricuspid valve in its native state, the right atriotomy was closed with 4-0 prolene (Figure 2B). Closure of the atriotomy was necessary to create a closed system that could sustain right ventricular pressure even after the induction of FTR. Without this step, increases in right ventricular pressure would result in leakage of air through the tricuspid valve and loss of pressure in the right ventricle. The right ventricular pressure was then increased from 30 mmHg to

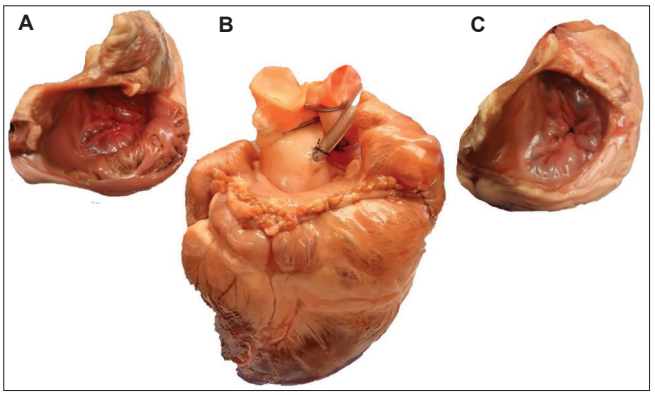

Figure 2. Development of functional tricuspid regurgitation (FTR). Representative images at each stage of development of the *ex vivo* model of FTR. (A) View of the native (control) tricuspid valve through a right atriotomy, with residual right atrial tissue retracted laterally. (B) Closure of the right atriotomy with 4-0 prolene and sustained pressurization of the right ventricle to 100 mmHg. (C) View of the regurgitant tricuspid valve with residual right atrial tissue excised.

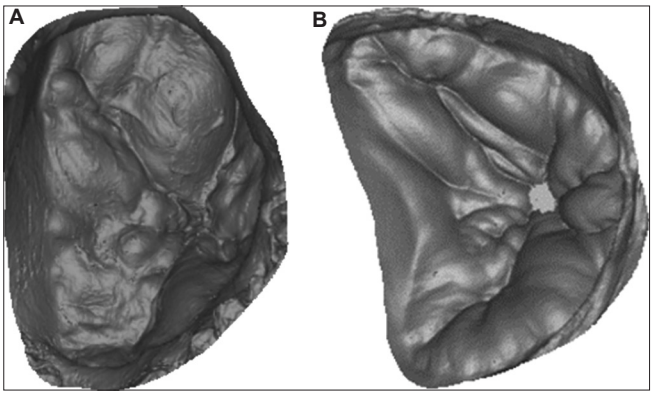

Figure 3. Representative 3D light scanner images of the tricuspid valve in the native (control) state (A), and after inducing functional tricuspid regurgitation with sustained pneumatic pressurization (B).

DOI: https://doi.org/10.36922/jctr.24.00003

100 mmHg, which mimics the right ventricular overload seen in FTR from left-sided valvular pathology. Right ventricular pressure was sustained at 100 mmHg for 3 h, with the intent of creating progressive annular and ventricular enlargement and inducing FTR. Throughout the 3-h period of sustained right ventricle pressurization, hydration of the tissues was ensured by periodically adding a small amount of fluid to the right ventricle, thus humidifying the air and maintaining the integrity of the tricuspid valve complex. Dampened towels were also applied to the exterior surface of the heart. After 3 h, the right atrium was excised to allow for optimal visualization of the tricuspid valve apparatus, and the tricuspid valve was imaged in its regurgitant state with the 3D light scanner (Figure 2C).

2.4. Outcomes

The primary outcomes of interest were tricuspid annular dimensions, including annular circumference, diameter, and area. Secondary outcomes were measures of leaflet geometry, including tenting height, angle, and area. For the model of FTR, the effective regurgitant orifice area was also measured and was defined as the area of visible malcoaptation. The annular diameter was measured in the minor axis, defined as the distance from the mid-septal leaflet to the opposite point on the annulus, and the major axis, defined as the greatest distance perpendicular to the minor axis (Figure 4A). Tenting height was defined as the maximum distance from the annular plane to the point of coaptation (Figure 4B). The tenting angle was measured as the angle between the annular plane and the septal leaflet. The tenting area was defined in the minor axis and was calculated by measuring the area between the annular plane and tricuspid leaflets. The tenting volume was defined as the volume between the annular plane and the tricuspid leaflets and was measured using a custom Python script. The Python script calculated tenting volume by dividing the valve into 100 slices along the X- and Y-axes below the annular plane, calculating the area of each slice, multiplying by the distance to the following slice, and summing these areas. The script then rotated the valve slightly for a total of 100 rotations, and the same process was repeated. After all rotations were completed, the average of all 100 tenting volumes was calculated to generate a final result.

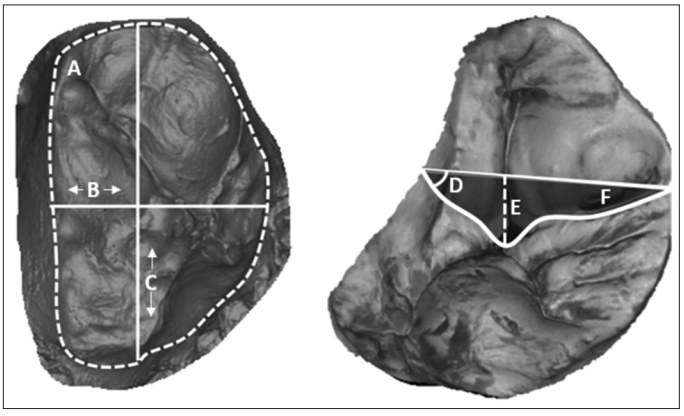

Figure 4. Geometric measurements sampled from 3D-reconstructed images of the tricuspid valve, including annular circumference and area (A), minor axis diameter (B), major axis diameter (C), tenting angle (D), tenting height (E), and tenting area (F).

2.5. Clinical validation

To compare the native geometry of the swine and human tricuspid valve and to validate the FTR model, the *ex vivo* native and FTR models were compared to publishe transesophageal echocardiographic (TEE) measurements from non-diseased (control) and FTR patients. Publications were selected if their methodology was well-described, and measurements were sampled in planes similar to those described above [11-13].

2.6. Statistical analysis

Comparisons were first made between the native and regurgitant *ex vivo* model and subsequently between the *ex vivo* model and *in vivo* echocardiographic data. Non-parametric testing was considered given the small sample size, but non-parametric comparisons between the *ex vivo* model and *in vivo* echocardiographic data were not possible as we did not have access to the underlying data sets for literature reported *in vivo* echocardiographic data. We instead verified the normality of our data using the Shapiro–Wilk test. Paired *t*-tests were then used to compare measurements between the native and regurgitant *ex vivo* model, and Student's *t*-test was used to compare measurements between the *ex vivo* model and literature-reported *in vivo* echocardiographic data. Data analysis was performed using STATA/IC 17.0 (StataCorp LLC, College Station, TX, USA), and statistical significance was set to a p-value ≤ 0.05 for all tests.

3. Results

3.1. Ex vivo model

A total of 12 porcine hearts, weighing 310–428 g each, were employed in this study. When compared to geometric measurements from the native *ex vivo* heart, all annular dimensions increased significantly with sustained pneumatic pressurization of the right ventricle (Table 1). The annular circumference and area increased by 16% and 35%, respectively (circumference: 11.8 vs. 13.7 cm, p=0.012; area: 10.5 vs. 14.0 cm^2, p=0.011). Major and minor axis diameters both increased from baseline, with the most substantial change seen in the minor axis (minor: 2.5 vs. 3.4 cm, p=0.05; major: 3.9 vs. 4.3 cm, p=0.05). The circularity index decreased with sustained pressurization (1.5 vs. 1.3, p=0.02), indicating a more circular annulus. When evaluating leaflet geometry, sustained pneumatic pressurization resulted in increased tethering of the anterior leaflet (Table 2), as evidenced by a significant increase in anterior leaflet angle (24° vs. 41°, p=0.008). Similarly, the *ex vivo* model of FTR yielded larger tenting height (8.0 vs. 11.5 mm, p=0.037), tenting area (1.0 vs. 2.0 cm^2, p=0.05), and tenting volume (3.4 vs. 7.4 cm^3, p=0.015) relative to baseline measurements. There was no significant change in septal leaflet tethering (31° vs. 30°, p=0.66). Minimal malcoaptation was present at baseline, as represented by a negligible effective regurgitant orifice area, but increased substantially after sustained pressurization (8.1 vs. 40.1 mm^2, p<0.001).

DOI: https://doi.org/10.36922/jctr.24.00003

Table 1. Comparison of clinical and *ex vivo* model annular dimensions

Annular measurements	Control	FTR	*P*-value
Annular circumference (cm)			
Ex vivo	11.8 (0.9)	13.7 (0.7)	0.01*
Clinical[a]	11 (1.5)	14 (3.8)	0.04*
P-value	0.21	0.85	
Annular area (cm^2)			
Ex vivo	10.5 (1.3)	14.1 (1.5)	0.01*
Clinical[a]	10.2 (2)	15 (5)	<0.01*
P-value	0.72	0.66	
Major axis diameter (cm)			
Ex vivo	3.9 (0.2)	4.3 (0.3)	0.05*
Clinical[a]	3.8 (0.4)	4.3 (0.8)	<0.01*
P-value	0.55	>0.9	
Minor axis diameter (cm)			
Ex vivo	2.5 (0.4)	3.4 (0.5)	0.05*
Clinical[a]	3.1 (0.5)	3.9 (0.7)	<0.01*
P-value	<0.01*	0.10	
Circularity index			
Ex vivo	1.5 (0.2)	1.3 (0.2)	0.02*
Clinical[b]	1.3 (0.1)	1.1 (0.1)	<0.01*
P-value	0.07	0.13	

Notes: Geometric measurements of the tricuspid valve annulus in an *ex vivo* porcine model in its non-diseased (control) and regurgitant (FTR) state as compared to published (clinical) TEE measurements by: [a]Karamali *et al.*[11] (n=52); or [b]Ton-Nu *et al.*[13] (n=75). All results are reported as mean (standard deviation). In the *ex vivo* model, "control" measurements were taken from the native tricuspid valve before inducing FTR. In the clinical data, "control" measurements were sampled from patients without FTR. Minor axis diameter was measured as a normal line from the mid-septal leaflet to the lateral wall. The major axis diameter was measured perpendicular to the minor axis at the point of maximum length. *$P \leq 0.05$.
Abbreviation: FTR: Functional tricuspid regurgitation.

Table 2. Comparison of clinical and *ex vivo* model leaflet geometry

Leaflet measurements	Control	FTR	*P*-value
Anterior leaflet angle			
Ex vivo	24 (7)	41 (9)	0.008*
Clinical[a]	10 (1)	25 (10)	0.003*
P-value	<0.001*	<0.001*	
Septal leaflet angle			
Ex vivo	31 (11)	30 (6)	0.66
Clinical[a]	12 (1)	22 (9)	<0.001*
P-value	<0.001*	0.040*	
Tenting height (mm)			
Ex vivo	8.0 (3.0)	11.5 (2.5)	0.037*
Clinical[a]	5.2 (1.8)	7.8 (3.4)	<0.001*
P-value	0.001*	0.013*	
Tenting area (cm^2)			
Ex vivo	1.0 (0.5)	2.0 (0.6)	0.05*
Clinical[a]	0.5 (0.3)	1.7 (1.2)	<0.001*
P-value	<0.001*	0.55	
Tenting volume (cm^3)			
Ex vivo	3.4 (1.4)	7.4 (1.4)	0.015*
Clinical[a]	1.1 (0.7)	3.0 (1.9)	<0.001*
P-value	<0.001*	<0.001*	
Effective regurgitant orifice area (mm^2)			
Ex vivo	-	40.1 (26.6)	-
Clinical[b]	-	22 (14)	-
P-value	-	0.049*	

Notes: Geometric measurements of the tricuspid valve leaflets in an *ex vivo* porcine model in its non-diseased (control) and regurgitant (FTR) state as compared to published (clinical) TEE measurements by: [a]Karamali *et al.*[11] (n=52); or [b]Florescu *et al.*[12] (n=58). All results are reported as mean (standard deviation). In the *ex vivo* model, "control" measurements were taken from the native tricuspid valve before inducing FTR. In the clinical data, "control" measurements were sampled from patients without FTR. Tenting height, area, and angle were measured in the septal-lateral plane. *$P \leq 0.05$.
Abbreviation: FTR: Functional tricuspid regurgitation.

3.2. Comparison with human echocardiographic data

When comparing the measurements obtained from the *ex vivo* porcine model to the *in vivo* human echocardiographic data, all annular measurements were comparable with the exception of baseline minor axis diameter, which was smaller in the *ex vivo* model (2.5 vs. 3.1 cm, p=0.007). Notably, after inducing FTR in the *ex vivo* model, the minor axis measurements were similar to those in humans with FTR (3.4 vs. 3.9 cm, p=0.10). When evaluating leaflet geometry, however, the majority of measurements from the *ex vivo* model differed from human echocardiographic data. At baseline, porcine leaflet geometry in the *ex vivo* model had steeper leaflet angles than those seen in normal humans (anterior: 24° vs. 10°, p<0.001, septal: 31° vs. 12°, p<0.001).

This translated into larger tenting height (8.0 vs. 5.2 mm, P = 0.001), area (1.0 vs. 0.5 cm^2, P < 0.001), and volume (3.4 vs. 1.1 cm^3, P < 0.001) relative to human measurements. These differences persisted after inducing FTR, with the exception of the tenting area, which was comparable between the *ex vivo* model and human echocardiographic data (2.0 vs. 1.7, P = 0.55). Although tenting measurements were larger in the porcine model than in human TEE data, the direction and magnitude of changes were comparable when comparing control and FTR measurements. For example, although anterior leaflet tenting angles were larger in the *ex vivo* model than in humans for both control and FTR measurements, the angle increased by an average of 17° in the *ex vivo* model and 15° in human TEE data. Similarly, tenting height in the *ex vivo* model increased by approximately 3.5 mm after sustained pressurization, as compared to a 2.6 mm increase in human TEE data.

4. Discussion

The objective of this study was to develop a simple, inexpensive, and reproducible porcine model of FTR for testing novel surgical and transcatheter interventions. We found that sustained pneumatic pressurization of the right ventricle results in geometric alterations that was comparable to those reported in the literature, including annular dilation and leaflet tethering.

After several hours of sustained right ventricular pressures at 100 mmHg, the mean tricuspid valve annular area increased from 10.5 to 14.1 cm^2 – an increase of nearly 35%. The majority of dilation occurred in the septolateral, or minor axis, corresponding to selective dilatation of the free wall of the right ventricle. These patterns are consistent with the geometric

DOI: https://doi.org/10.36922/jctr.24.00003

alterations reported in humans with FTR, wherein the normally saddle-shaped tricuspid annulus dilates and becomes more circular [14-17]. We also observed alterations in the subvalvular apparatus of the tricuspid valve, with significant increases in the anterior leaflet angle, tenting height, tenting area, and tenting volume. Historically, the importance of the subvalvular anatomy of the tricuspid valve was not appreciated, and the emphasis was placed primarily on reducing the size of the tricuspid annulus to restore leaflet coaptation. Recent publications have emphasized the importance of residual leaflet tethering as a predictor of failure after tricuspid repair and have called for novel repair strategies that address both annular dilation and leaflet tethering [18-20]. Our *ex vivo* model of FTR incorporates both of these geometric alterations and thus offers a realistic platform for testing novel repair strategies.

When directly comparing geometric measurements between the *ex vivo* model and human TTE data, the majority of annular dimensions remained similar. These results are consistent with both *ex vivo* and *in vivo* reports of porcine tricuspid anatomy. In an evaluation of 119 porcine hearts, Waziri *et al.* demonstrated no difference in tricuspid annulus circumference or area compared to humans [21]. Similarly, Fawzy *et al.* evaluated the 3D geometry of the tricuspid annulus in anesthetized swine using sonomicrometry and described similar annular dimensions to humans [22]. These findings collectively demonstrate that the native porcine tricuspid valve reasonably approximates that of a human, justifying its future utilization in translational research.

Our data demonstrated that the subvalvular apparatus of the porcine tricuspid valve was not directly comparable to that of a human. At baseline, the porcine tricuspid valve had a narrower minor axis with steeper leaflet angles and greater tenting than that of a human. As such, many of these differences persisted after inducing FTR; the porcine valve had greater anterior and septal leaflet angles, tenting height, and tenting volume relative to human TTE data. Given that our annular measurements were comparable between the *ex vivo* model and human TTE data, the observed differences in subvalvular measurements likely reflect differences in anatomy between species rather than flaws in the *ex vivo* model itself. Surprisingly, no study has evaluated the differences in subvalvular anatomy between swine and humans, despite numerous translational studies being performed in porcine models. Despite these differences, the strength of this model lies in the geometric alterations observed between the native and FTR states; although the subvalvular measurements were not identical between swine and humans, the directional and incremental changes between normal and diseased specimens were similar.

Furthermore, our model compares favorably to those described by other groups in terms of validity, simplicity, and cost. Adkins *et al.* induced FTR in ovine hearts by injecting 95% phenol around the annulus to create annular dilation, but the degree of dilation was not validated and there was no alteration of the subvalvular apparatus [3]. Stock *et al.* isolated porcine tricuspid valve complexes and mounted them on an adjustable supporting device [4]. This allowed for replication of the geometric changes observed with FTR but provided a rigid model with fixed geometry even after the application of surgical repairs. Perhaps the most comparable model was proposed by Maisano *et al.*, wherein a closed, pressurized circuit was developed using a centrifugal pump, and the porcine right ventricle was dilated with sustained pressure [23]. The authors used radiopaque markers and fluoroscopy to document the occurrence of tricuspid annular dilation, papillary muscle displacement, and induction of FTR after pressurizing the right ventricle. Our model requires fewer resources; the pneumatic pump and 3D light scanner required for this model are both commercially available and comparatively inexpensive. Furthermore, the 3D geometry of our model was directly compared to normal and diseased human TTE data in this study, whereas the model suggested by Maisano *et al.* solely describes the geometric changes relative to the baseline.

We acknowledge that this model has several limitations. First, this is a static representation of the tricuspid valve at peak systole and cannot be used to evaluate valvular anatomy in diastole. We believe that the mid-systolic phase of the cardiac cycle is the most clinically relevant to capture when evaluating the effectiveness of repair strategies for FTR. Tricuspid stenosis is exceedingly uncommon and is unlikely to occur with the application of repair strategies for FTR, where the annulus has already dilated from baseline. Even so, the diastolic performance of novel repairs would need to be examined *in vivo* or with a dynamic, pulsatile *ex vivo* model. Second, preservation of the pericardium was not possible due to the manner in which the porcine hearts were harvested. Assessment of pericardial contributions to valvular geometry would be better assessed with an *in vivo* model. Furthermore, we employed a pneumatic model for pressurizing the right ventricle, potentially resulting in different mechanics of valve closure than those observed with blood. The pneumatic model also limits our ability to assess the right ventricle, as the structured light scanner used in this model is restricted to the assessment of surface-level anatomy. Qualitative assessment of the right ventricle in the *ex vivo* model before and after sustained pneumatic pressurization suggests right ventricular dilatation as the source of increased tenting angles with the induction of FTR, but this was not quantifiable. Similarly, the individual contribution of constituent elements of the tricuspid valve was not assessed in this research. Previous research has implicated the transition between the papillary muscle and chordae tendinae as a potential origin of valve deformation [24,25], which may or may not be accurately represented by the *ex vivo* model proposed herein. Finally, as mentioned above, it is important to take into consideration the baseline differences in anatomy between swine and humans when interpreting results from this model. We observed modest differences in subvalvular anatomy between swine and human data. As such, any subvalvular geometric measurements sampled in the *ex vivo* FTR model should be interpreted in reference to *ex vivo* native measurements, and not to normal human TTE data.

5. Conclusion

The *ex vivo* porcine model of FTR characterized in this study demonstrates consistent annular dilation and leaflet

DOI: https://doi.org/10.36922/jctr.24.00003

tethering that mimics the direction and magnitude of geometric alterations observed in humans with FTR. This model offers a simple, reproducible, and cost-effective option for testing and optimizing novel interventions for FTR before *in vivo* or clinical studies.

Acknowledgments

None.

Funding

This research was funded, in part, by the American Heart Association (Award #908805) and the American Association for Thoracic Surgery Summer Intern Scholarship.

Conflict of Interest

The authors have no competing interests to disclose.

Ethics Approval and Consent to Participate

This study did not involve human subjects and was therefore exempt from IRB approval.

Consent for Publication

Not applicable.

Availability of Data

Data are available from the corresponding author upon reasonable request.

References

[1] Topilsky Y, Khanna A, Le Tourneau T, Park S, Michelena H, Suri R, *et al*. Clinical Context and Mechanism of Functional Tricuspid Regurgitation in Patients with and without Pulmonary Hypertension. Circ Cardiovasc Imaging 2012;5:314-23.
doi: 10.1161/CIRCIMAGING.111.967919

[2] Gammie JS, Chu MW, Falk V, Overbey JR, Moskowitz AJ, Gillinov M, *et al*. Concomitant Tricuspid Repair in Patients with Degenerative Mitral Regurgitation. N Engl J Med 2022;386:327-39.
doi: 10.1056/NEJMoa2115961

[3] Adkins A, Aleman J, Boies L, Sako E, Bhattacharya S. Force Required to Cinch the Tricuspid Annulus: An *Ex-vivo* Study. J Heart Valve Dis 2015;24:644-52.

[4] Stock S, Bohm H, Scharfschwerdt M, Richardt D, Meyer-Saraei R, Tsvelodub S, *et al*. *Ex Vivo* Hydrodynamics after Central and Paracommissural Edge-to-Edge Technique: A Further Step Toward Transcatheter Tricuspid Repair? J Thorac Cardiovasc Surg 2018;155:949-55.
doi: 10.1016/j.jtcvs.2017.10.068

[5] Amini Khoiy K, Biswas D, Decker TN, Asgarian KT, Loth F, Amini R. Surface Strains of Porcine Tricuspid Valve Septal Leaflets Measured in *Ex Vivo* Beating Hearts. J Biomech Eng 2016;138:111006.
doi: 10.1115/1.4034621

[6] Amini Khoiy K, Asgarian KT, Loth F, Amini R. Dilation of Tricuspid Valve Annulus Immediately after Rupture of Chordae Tendineae in *Ex-Vivo* Porcine Hearts. PLoS One 2018;13:e0206744.
doi: 10.1371/journal.pone.0206744

[7] Nguyen YN, Tay EL, Kabinejadian F, Ong CW, Ismail M, Leo HL. Ventricular Vortex Loss Analysis Due to Various Tricuspid Valve Repair Techniques: An *Ex Vivo* Study. Am J Physiol Heart Circ Physiol 2019;317:H1312-27.
doi: 10.1152/ajpheart.00150.2019

[8] Salurso E, Jaworek M, Perico F, Frigelli M, Romagnoni C, Contino M, *et al*. Morphometric Characterization of an *Ex Vivo* Porcine Model of Functional Tricuspid Regurgitation. Ann Biomed Eng 2022;51:715-25.
doi: 10.1007/s10439-022-03080-2

[9] Pasrija C, Quinn R, Ghoreishi M, Eperjesi T, Lai E, Gorman RC, *et al*. A Novel Quantitative *Ex Vivo* Model of Functional Mitral Regurgitation. Innovations (Phila) 2020;15:329-37.
doi: 10.1177/1556984520930336

[10] Crick SJ, Sheppard MN, Ho SY, Gebstein L, Anderson RH. Anatomy of the pig Heart: Comparisons with Normal Human Cardiac Structure. J Anat 1998;193:105-19.
doi: 10.1046/j.1469-7580.1998.19310105.x

[11] Karamali F, Hosseini S, Shojaeifard M, Mohammadi K, Kaviani R, Rezaei Y, *et al*. Tricuspid Valve Geometry in Patients with Functional Tricuspid Regurgitation: A Three-Dimensional Echocardiographic Study. Echocardiography 2020;37:867-75.
doi: 10.1111/echo.14747

[12] Florescu DR, Muraru D, Florescu C, Volpato V, Caravita S, Perger E, *et al*. Right Heart Chambers Geometry and Function in Patients with the Atrial and the Ventricular Phenotypes of Functional Tricuspid Regurgitation. Eur Heart J Cardiovasc Imaging 2022;23:930-40.
doi: 10.1093/ehjci/jeab211

[13] Ton-Nu TT, Levine RA, Handschumacher MD, Dorer DJ, Yosefy C, Fan D, *et al*. Geometric determinants of Functional Tricuspid Regurgitation: Insights from 3-Dimensional Echocardiography. Circulation 2006;114:143-9.
doi: 10.1161/CIRCULATIONAHA.106.611889

[14] Badano LP, Hahn R, Rodríguez-Zanella H, Araiza Garaygordobil D, Ochoa-Jimenez RC, Muraru D. Morphological Assessment of the Tricuspid Apparatus and Grading Regurgitation Severity in Patients with Functional Tricuspid Regurgitation: Thinking Outside the Box. JACC Cardiovasc Imaging 2019;12:652-64.
doi: 10.1016/j.jcmg.2018.09.029

[15] Badano LP, Agricola E, Perez de Isla L, Gianfagna P,

Zamorano JL. Evaluation of the Tricuspid Valve Morphology and Function by Transthoracic Real-Time Three-Dimensional Echocardiography. Eur J Echocardiogr 2009;10:477-84.
doi: 10.1093/ejechocard/jep044

[16] Fukuda S, Saracino G, Matsumura Y, Daimon M, Tran H, Greenberg NL, *et al*. Three-Dimensional Geometry of the Tricuspid Annulus in Healthy Subjects and in Patients with Functional Tricuspid Regurgitation: A Real-Time, 3-Dimensional Echocardiographic Study. Circulation 2006;114 1 Suppl: I492-8.
doi: 10.1161/CIRCULATIONAHA.105.000257

[17] Fukuda S, Gillinov AM, Song JM, Daimon M, Kongsaerepong V, Thomas JD, *et al*. Echocardiographic Insights into Atrial and Ventricular Mechanisms of Functional Tricuspid Regurgitation. Am Heart J 2006;152:1208-4.
doi: 10.1016/j.ahj.2006.07.027

[18] Fukuda S, Gillinov AM, McCarthy PM, Stewart WJ, Song JM, Kihara T, *et al*. Determinants of Recurrent or Residual Functional Tricuspid Regurgitation after Tricuspid Annuloplasty. Circulation 2006;114 1 Suppl: I582-7
doi: 10.1161/CIRCULATIONAHA.105.001305

[19] Kabasawa M, Kohno H, Ishizaka T, Ishida K, Funabashi N, Kataoka A, *et al*. Assessment of Functional Tricuspid Regurgitation using 320-Detector-Row Multislice Computed Tomography: Risk Factor Analysis for Recurrent Regurgitation after Tricuspid Annuloplasty. J Thorac Cardiovasc Surg 2014;147:312-20.
doi: 10.1016/j.jtcvs.2012.11.017

[20] Maslow A, Abisse S, Parikh L, Apruzzese P, Cilia L, Gleason P, *et al*. Echocardiographic Predictors of Tricuspid Ring Annuloplasty Repair Failure for Functional Tricuspid Regurgitation. J Cardiothorac Vasc Anesth 2019;33:2624-33.
doi: 10.1053/j.jvca.2019.05.043

[21] Waziri F, Lyager Nielsen S, Michael Hasenkam J. Porcine Tricuspid Valve Anatomy and Human Compatibility: Relevance for Preclinical Validation of Novel Valve Interventions. J Heart Valve Dis 2016;25:596-605.

[22] Fawzy H, Fukamachi K, Mazer CD, Harrington A, Latter D, Bonneau D, *et al*. Complete Mapping of the Tricuspid Valve Apparatus using Three-Dimensional Sonomicrometry. J Thorac Cardiovasc Surg 2011;141:1037-43.
doi: 10.1016/j.jtcvs.2010.05.039

[23] Maisano F, Taramasso M, Guidotti A, Redaelli A, Fiore GB, Baroni G, *et al*. Simulation of Functional Tricuspid Regurgitation using an Isolated Porcine Heart Model. J Heart Valve Dis 2011;20:657-63.

[24] Madhurapantula RS, Krell G, Morfin B, Roy R, Lister K, Orgel JP. Advanced Methodology and Preliminary Measurements of Molecular and Mechanical Properties of Heart Valves under Dynamic Strain. Int J Mol Sci 2020;21:763.
doi: 10.3390/ijms21030763

[25] Roy R, Warren E Jr., Xu Y, Yow C, Madhurapantula RS, Orgel JP, *et al*. Functional Grading of a Transversely Isotropic Hyperelastic Model with Applications in Modeling Tricuspid and Mitral Valve Transition Regions. Int J Mol Sci 2020;21:6503.
doi: 10.3390/ijms21186503

DOI: https://doi.org/10.36922/jctr.24.00003